Title
Photochemical production and evolution of selected C2-C5 alkyl nitrates in tropospheric air influenced by Asian outflow

Journal
Journal of Geophysical Research: Atmospheres, 108(20)

ISSN
0148-0227

Authors
Simpson, IJ
Blake, NJ
Blake, DR
et al.

Publication Date
2003-10-27

DOI
10.1029/2002jd002830

Photochemical production and evolution of selected C_2-C_5 alkyl nitrates in tropospheric air influenced by Asian outflow

Isobel J. Simpson,[1] Nicola J. Blake,[1] Donald R. Blake,[1] Elliot Atlas,[2] Frank Flocke,[2] James H. Crawford,[3] Henry E. Fuelberg,[4] Christopher M. Kiley,[4] Simone Meinardi,[1] and F. Sherwood Rowland[1]

Received 8 August 2002; revised 16 November 2002; accepted 25 November 2002; published 18 September 2003.

[1] The photochemical production and evolution of six C_2-C_5 alkyl nitrates (ethyl-, 1-propyl-, 2-propyl-, 2-butyl-, 2-pentyl-, and 3-pentyl nitrate) was investigated using selected data from 5500 whole air samples collected downwind of Asia during the airborne Transport and Chemical Evolution over the Pacific (TRACE-P) field campaign (February–April 2001). Air mass age was important for selecting appropriate field data to compare with laboratory predictions of C_5 alkyl nitrate production rates. In young, highly polluted air masses, the ratio between the production rates of 3-pentyl nitrate and 2-pentyl nitrate from *n*-pentane was 0.60–0.65. These measured ratios show excellent agreement with results from a field study in Germany (0.63 ± 0.06), and they agree better with predicted ratios from older laboratory kinetic studies (0.63–0.66) than with newer laboratory results (0.73 ± 0.08). TRACE-P samples that did not show influence from marine alkyl nitrate sources were used to investigate photochemical alkyl nitrate evolution. Relative to 2-butyl nitrate/*n*-butane, the measured ratios of ethyl nitrate/ethane and 2-propyl nitrate/propane showed notable deviations from modeled values based on laboratory kinetic data, suggesting additional Asian sources of their alkyl peroxy radical precursors. By contrast, the measured ratios of 1-propyl-, 2-pentyl-, and 3-pentyl nitrate to their respective parent hydrocarbons were fairly close to modeled values. The 1-propyl nitrate findings contrast with field studies in North America, and suggest that air downwind of Asia was not significantly impacted by additional 1-propyl nitrate precursors. The sensitivity of modeled photochemical processing times to hydroxyl radical concentration, altitude, city ventilation times, and dilution is discussed. *INDEX TERMS:* 0315 Atmospheric Composition and Structure: Biosphere/atmosphere interactions; 0317 Atmospheric Composition and Structure: Chemical kinetic and photochemical properties; 0322 Atmospheric Composition and Structure: Constituent sources and sinks; 0365 Atmospheric Composition and Structure: Troposphere—composition and chemistry; 0368 Atmospheric Composition and Structure: Troposphere—constituent transport and chemistry; *KEYWORDS:* alkyl nitrates, photochemical production, evolution, Asian outflow, TRACE-P

Citation: Simpson, I. J., N. J. Blake, D. R. Blake, E. Atlas, F. Flocke, J. H. Crawford, H. E. Fuelberg, C. M. Kiley, S. Meinardi, and F. S. Rowland, Photochemical production and evolution of selected C_2-C_5 alkyl nitrates in tropospheric air influenced by Asian outflow, *J. Geophys. Res.*, *108*(D20), 8808, doi:10.1029/2002JD002830, 2003.

1. Introduction

[2] Alkyl nitrates ($RONO_2$) have a relatively low reactivity compared with other components of reactive odd nitrogen (NO_y), which allows them to serve as a reservoir for the long-range transport of nitrogen oxides (NO_x = NO + NO_2). Within the troposphere the concentration of NO_x controls ozone (O_3) production [*Talbot et al.*, 2000], and alkyl nitrates can be used as tracers of photochemical O_3 production from anthropogenic precursors [*Flocke et al.*, 1998]. Whereas studies of continental air masses have shown that alkyl nitrates typically comprise less than 10% of NO_y [*Buhr et al.*, 1990; *Ridley et al.*, 1990; *Flocke et al.*, 1991; *Shepson et al.*, 1993], alkyl nitrates have been found to comprise a large component (20–80%) of total NO_y in the equatorial marine boundary layer over the Pacific [*Talbot et al.*, 2000; *Blake et al.*, 2003].

[3] Alkyl nitrate sources include marine emissions [*Walega et al.*, 1992; *Atlas et al.*, 1993; *Atlas and Ridley*, 1996; *Hess et al.*, 1996; *Blake et al.*, 1999, 2003; *Chuck et al.*, 2002] and photochemical production from the oxidation of parent hydrocarbons [*Darnall et al.*, 1976; *Atkinson et al.*, 1982; *Roberts*, 1990; *Atkinson et al.*, 1995; *Arey et al.*, 2001]. In addition, biomass burning has recently been

[1]Department of Chemistry, University of California-Irvine, Irvine, California, USA.
[2]National Center for Atmospheric Research, Boulder, Colorado, USA.
[3]NASA Langley Research Center, Hampton, Virginia, USA.
[4]Florida State University, Tallahassee, Florida, USA.

0148-0227/03/2002JD002830

identified as a source of C_1-C_4 alkyl nitrates [*Simpson et al.*, 2002]. Although methyl nitrate ($MeONO_2$) was the most abundant alkyl nitrate released from Australian savanna burning, biomass burning likely has only a small impact on the global $MeONO_2$ budget. The importance of the marine alkyl nitrate source decreases with increasing carbon number, and marine emissions are only a minor source of C_4 alkyl nitrates [*Blake et al.*, 2003]. The marine source of C_5 alkyl nitrates is also likely to be small. In photochemical alkyl nitrate production, whereas the branching ratios leading to alkyl nitrate formation increase with increasing carbon number [*Atkinson et al.*, 1982; *Arey et al.*, 2001], the ambient concentrations of parent *n*-alkanes decrease with increasing carbon number. Together, the net effect of these factors leads to a maximum abundance of C_3-C_4 alkyl nitrates from the photochemical source, in particular 2-propyl- and 2-butyl nitrate.

[4] Here we use alkyl nitrate measurements collected during the airborne NASA Transport and Chemical Evolution over the Pacific (TRACE-P) field campaign (February–April 2001) to investigate the photochemical production, transport, and chemical evolution of alkyl nitrates in tropospheric air influenced by Asian outflow. We developed the capability to accurately measure C_5 alkyl nitrates shortly before the TRACE-P mission, and the TRACE-P data set provides a timely opportunity to compare field measurements of photochemical C_5 alkyl nitrate production rates with newly published values from laboratory kinetic studies. In photochemical alkyl nitrate production the ratio of a daughter alkyl nitrate to its parent hydrocarbon can be used to determine the extent of photochemical processing within an air mass [*Bertman et al.*, 1995; *Flocke et al.*, 1998; *Roberts et al.*, 1998; *Stroud et al.*, 2001]. Ratios of daughter alkyl nitrates to their parent hydrocarbons were used to investigate alkyl nitrate sources, evolution, and air mass age in tropospheric air samples collected between altitudes of 150 m and 12 km.

2. Experiment

[5] The alkyl nitrate measurements presented in this paper result from a collaboration between the University of California, Irvine (UCI) and the National Center for Atmospheric Research (NCAR). During TRACE-P we measured six C_2-C_5 alkyl nitrates: ethyl nitrate ($EtONO_2$), 1-propyl nitrate (1-$PrONO_2$), 2-propyl nitrate (2-$PrONO_2$), 2-butyl nitrate (2-$BuONO_2$), 2-pentyl nitrate (2-$PeONO_2$), and 3-pentyl nitrate (3-$PeONO_2$). The measurements were made using a combination of airborne whole air sampling, followed by laboratory gas chromatography (GC) analysis with electron capture detection (ECD). Although we also measured $MeONO_2$ during the TRACE-P mission, its photochemical production from methane is extremely slow and we do not consider the photochemical production and evolution of $MeONO_2$ in this paper.

[6] The whole air samples were collected aboard NASA DC-8 and P-3B research aircraft during 38 science flights of the TRACE-P field campaign (24 February–10 April 2001). The air samples were collected at altitudes between 150 m and 12 km over the western and central Pacific Ocean, with main deployment bases in Hong Kong (22°N, 114°E) and Yokota Air Force Base, Japan (36°N, 140°E). A detailed overview of the sampling area, including flight tracks for both aircraft, is given by *Jacob et al.* [2003]. Individual air samples were collected in 2-L stainless steel canisters each equipped with a stainless steel bellows valve. Prior to the mission, the canisters were conditioned and evacuated, and 10 Torr of degassed, distilled water was added into each canister to quench active surface sites. The air samples were collected roughly every 3–7 min during horizontal flight legs and every 1–3 min during ascents and descents. Horizontal sampling times were approximately 1 min and correspond to a sampling distance of about 12 km. Approximately 160 air samples were collected per flight aboard the DC-8, and 140 were collected aboard the P-3B.

[7] After each flight, the filled canisters were transported back to the UCI laboratory. Within 10 days of being collected, each air sample was analyzed for alkyl nitrates and more than 50 other trace gases comprising nonmethane hydrocarbons (NMHCs), halocarbons, and sulfur compounds. The same canisters were reused during the course of the mission, and two identical analytical systems (sharing the same standards) were operated simultaneously in order to improve the canister turn-around time. Because it takes a few days for the analytical systems to equilibrate, they were operated 24 hours a day throughout the mission in order to generate an internally consistent data set.

[8] The reader is referred to *Colman et al.* [2001] for a detailed description of our analytical procedure. Briefly, to analyze each TRACE-P whole air sample, the less volatile components contained within 1520 ± 1 cm^3 (STP) of canister air (i.e., alkyl nitrates, NMHCs, halocarbons, and DMS) were preconcentrated by passing the air through tubing immersed in a liquid nitrogen bath. The components were revolatilized using a hot water bath and then reproducibly split into five streams, with each stream directed to a different column-detector combination. We have found that the split ratios are highly reproducible as long as the specific humidity of the air is greater than 0.3 kPa at 298 K, which we ensure by the addition of 10 Torr (1.3 kPa) of water into each canister (see above).

[9] The C_2-C_5 alkyl nitrates were analyzed using two of the five column-detector combinations. The first column-detector combination (abbreviated as "Restek1701/ECD") was a RESTEK 1701 column (60 m, 0.25 mm I.D., 0.50 μm film thickness) output to an ECD. The second combination ("DB5-Restek1701/ECD") was a DB-5 column (J&W, 30 m, 0.25 mm I.D., 1 μm film thickness) connected in series to a RESTEK 1701 column (5 m, 0.25 mm I.D., 0.5 μm film thickness) and output to an ECD. The Restek1701/ECD and DB5-Restek1701/ECD combinations received 7.2 and 6.8% of the sample flow, respectively, and were housed in separate GCs (HP-6890). For the C_2-C_4 alkyl nitrates the mixing ratios determined from both column-detector combinations agreed very well and were averaged to give a single mixing ratio for each sample. The slope calculated for both combinations differed from the 1:1 line by 1% for $EtONO_2$, 2% for 1-$PrONO_2$, 2% for 2-$PrONO_2$, and 4% for 2-$BuONO_2$. In each case the r^2 value exceeded 0.99 and the intercept was between 0.01 and 0.04 pptv. For the C_5 alkyl nitrates, the two combinations showed very good agreement for 2-$PeONO_2$ (slope = 1.04; r^2 = 0.98) and fair agreement for 3-$PeONO_2$ (slope = 1.22; r^2 = 0.98). The Restek1701/ECD results were not used for 3-$PeONO_2$ because they

showed a poorer correlation with the 2-$BuONO_2$ mixing ratios than did the DB5-Restek1701/ECD results. For similar reasons, the DB5-Restek1701/ECD results were not used for 2-$PeONO_2$.

[10] The alkyl nitrate measurements were calibrated using two whole air working standards that were analyzed every four samples and have been previously calibrated against a synthetic standard prepared at NCAR. The alkyl nitrate measurement precision is conservatively 2% for mixing ratios above 5 parts per trillion by volume (pptv) and 10% for mixing ratios below 5 pptv. The accuracy of the alkyl nitrate measurements is 10–20%, and the alkyl nitrate detection limit is 0.01 pptv.

3. Alkyl Nitrate Chemistry

3.1. Photochemical Production of Alkyl Nitrates

[11] The photochemical production of alkyl nitrates in the troposphere is initiated by the oxidation of parent hydrocarbons (RH) by the hydroxyl radical (OH) leading to the formation of parent alkyl peroxy radicals (RO_2):

$$RH + OH\cdot \rightarrow R\cdot + H_2O \qquad k_1, \alpha_1 \qquad (1)$$

$$R\cdot + O_2 \rightarrow RO_2\cdot \qquad k_2 \qquad (2)$$

where k_1 and k_2 are reaction rate constants and the branching ratio α_1 quantifies the fractional yield of a specific parent RO_2. For example, for C_3–C_4 parent *n*-alkanes (propane, *i*-butane, and *n*-butane), equation (1) gives rise to two possible RO_2 isomers, depending on which hydrogen is abstracted by OH. (The group rate constant for hydrogen atom extraction from alkanes is larger for a tertiary carbon than a secondary carbon and larger for a secondary carbon than a primary carbon (Table 1).) The branching ratio α_1 is calculated using the group rate constants and group substituent factors derived by *Atkinson* [1987] and revised by *Kwok and Atkinson* [1995] (Table 1).

[12] At NO mixing ratios greater than about 30–40 pptv the subsequent reaction of RO_2 with NO dominates over RO_2 reaction with nitrogen dioxide (NO_2), hydroperoxy radicals (HO_2), or other RO_2 radicals [*Logan*, 1985; *Finlayson-Pitts and Pitts*, 2000]. The reaction of RO_2 with NO has two possible outcomes (equations (3a)–(3b)), one of which leads to the formation of a daughter alkyl nitrate (equation (3b)):

$$RO_2 + NO \rightarrow RO + NO_2 \qquad k_{3a}, 1-\alpha_2 \qquad (3a)$$

$$RO_2 + NO \rightarrow RONO_2 \qquad k_{3b}, \alpha_2 \qquad (3b)$$

where k_{3a} and k_{3b} are reaction rate constants and the branching ratio α_2 quantifies the fractional yield of the daughter alkyl nitrate from the reaction of RO_2 with NO:

$$\alpha_2 = k_{3b}/(k_{3a} + k_{3b}). \qquad (4)$$

Alkyl nitrates are a minor product of RO_2 + NO reaction. In laboratory studies, α_2 has been found to range from 0.006 for $EtONO_2$ [*Ranschaert et al.*, 2000] to 0.126 for 3-$PeONO_2$ [*Arey et al.*, 2001]. In addition to increasing with increasing carbon number, the magnitude of α_2 is also a function of temperature and pressure [*Atkinson et al.*, 1982; *Carter and Atkinson*, 1989].

Table 1. Structure-Activity Parameters for Hydrogen Atom Abstraction From -CH_3, -CH_2-, and >CH- Groups in Alkane Molecules[a]

Source	k_{prim}	k_{sec}	k_{tert}	F(-CH_3)	F(-CH_2-)	F(>CH-)
Atkinson [1987]	0.144	0.838	1.83	1.00	1.29	1.29
Kwok and Atkinson [1995]	0.136	0.934	1.94	1.00	1.23	1.23

[a]Here, k_{prim}, k_{sec}, and k_{tert} are group rate constants for H-atom abstraction from -CH_3, -CH_2-, and >CH-, respectively (all *k* values are for 298 K and have units of 10^{-12} cm^3 $molec^{-1}$ s^{-1}); F(X) is the group substituent factor for substituent group X (F(-CH_3) is 1.00 by definition).

3.2. Photochemical Destruction of Alkyl Nitrates

[13] Alkyl nitrates are destroyed by photolysis or by reaction with OH:

$$RONO_2 + h\nu \rightarrow RO + NO_2 \qquad J_{RONO2} \qquad (5)$$

$$RONO_2 + OH \rightarrow \text{products} \qquad k_4 \qquad (6)$$

where J_{RONO2} and k_4 are the reaction rate constants for the loss of alkyl nitrates by photolysis and OH, respectively. Previous studies have found that the photolysis pathway is the dominant loss process for C_1–C_3 alkyl nitrates [*Roberts and Fajer*, 1989; *Clemitshaw et al.*, 1997; *Talukdar et al.*, 1997]. For example, *Talukdar et al.* [1997] calculated that reaction with OH can contribute approximately 20% of the total loss rate for $EtONO_2$ and 2-$PrONO_2$ and less than 10% for $MeONO_2$ (see *Talukdar et al.* [1997] for assumed conditions).

[14] The rate of $RONO_2$ destruction varies with altitude, season, and latitude. For example, J_{RONO2} is a function of both solar flux intensity (which increases with altitude) and absorption cross section (which decreases with altitude) [*Clemitshaw et al.*, 1997 and references therein; *Talukdar et al.*, 1997]. Overall, the higher solar flux intensities at higher altitudes cause J_{RONO2} to increase with height in the troposphere [*Talukdar et al.*, 1997]. For 1 April and 40°N, *Clemitshaw et al.* [1997] calculated that *J*-values for selected C_2–C_5 alkyl nitrates are more than a factor of two higher at 10 km than at the surface. By contrast, the reaction of $RONO_2$ with OH decreases with increasing altitude because of slower rate constants and lower OH concentrations. For conditions comparable to those encountered during TRACE-P (1 April, 40°N), the surface level lifetimes of the C_2–C_5 alkyl nitrates considered here range from 6 to 17 days (Table 2).

3.3. Alkyl Nitrate Evolution

[15] Assuming that OH reaction with the parent hydrocarbon is the rate-limiting step in photochemical alkyl nitrate formation, equations (1)–(3) and (5)–(6) can be simplified to sequential alkyl nitrate production and destruction [*Bertman et al.*, 1995]:

$$RH \rightarrow RONO_2 \qquad k_A, \beta \qquad (7)$$

$$RONO_2 \rightarrow \text{products} \qquad k_B \qquad (8)$$

Table 2. Kinetic Data for the Alkyl Nitrates Measured During TRACE-P[a]

	$RONO_2$ production				$RONO_2$ loss								
	k_1[b]		k_A		k_4[c]		k_4 [OH]		J[d]		k_B		Lifetime
Alkyl Nitrate	298 K	245 K	0 km	10 km	298 K	245 K	0 km	10 km	0 km	10 km	0 km	10 km	0 km
$EtONO_2$	0.254	0.12	0.22	0.04	0.49	n/a	0.43	n/a	0.24	0.55	0.67	n/a	17
1-$PrONO_2$	1.12	0.72	0.99	0.23	0.73	n/a	0.64	n/a	0.33	0.74	0.97	n/a	12
2-$PrONO_2$	1.12	0.72	0.99	0.23	0.49	n/a	0.43	n/a	0.57	1.27	1.00	n/a	12
2-$BuONO_2$	2.44	1.83	2.15	0.59	0.92*	n/a	0.81	n/a	0.47	1.06	1.28	n/a	9
2-$PeONO_2$	4.00	3.09	3.52	0.99	1.85*	n/a	1.63	n/a	0.46	1.04	2.09	n/a	6
3-$PeONO_2$	4.00	3.09	3.52	0.99	1.12*	n/a	0.99	n/a	0.44	1.01	1.43	n/a	8

[a]Units: 10^{-12} cm^3 $molec^{-1}$ s^{-1} for k_1 and k_4; 10^{-6} s^{-1} for k_A, k_B, k_4[OH], and J; days for lifetime. We emphasize that the 10 km J-values were calculated without applying temperature-dependent absorption cross-sections and are likely overestimated. Diurnally averaged [OH] of 8.8×10^5 and 3.2×10^5 molec cm^{-3} were used for calculations at 0 km and 10 km, respectively. "n/a" = not available.

[b]*Atkinson* [1997]. Although an average temperature of 230 ± 5 K was measured between 9.5 and 10.5 km during TRACE-P, we used 245 K to simulate upper tropospheric temperatures because temperature-dependent rate constants are only available over the restricted range 245–330 K.

[c]*Atkinson et al.* [1997]. Entries marked with an asterisk are from *Atkinson* [1990]. Temperature-dependent rate constants are only available over the restricted temperature range 290–380 K, and k_4 could not be calculated for upper tropospheric temperatures.

[d]Diurnal J-values were calculated using absorption cross-sections reported by *Roberts and Fajer* [1989] and conditions appropriate for TRACE-P (1 April; 40°N; ozone column = 350 Dobson Units; see text).

where $k_A = k_1[OH]$ and $k_B = J_{RONO2} + k_4[OH]$ are pseudo-first order rate constants, and the factor $\beta = \alpha_1\alpha_2$ takes into account the branching ratios that lead to the alkyl nitrate formation, assuming no peroxy radical self-reaction. The time evolution of a daughter alkyl nitrate to its parent hydrocarbon in an air mass can then be modeled by [*Bertman et al.*, 1995]:

$$\frac{[RONO_2]}{[RH]} = \frac{\beta k_A}{(k_B - k_A)}\left(1 - e^{(k_A - k_B)t}\right) \quad (9)$$

where the initial concentration of the alkyl nitrate is assumed to be zero.

[16] If we assume that photochemical losses are negligible compared to production (such as in very fresh air masses) and consider only chemical terms (i.e., dilution acts on each species equally and there is negligible contribution from marine alkyl nitrate sources), then the measured mixing ratios of two daughter alkyl nitrates i and j that originate from the same parent hydrocarbon are related by [*Flocke et al.*, 1998]:

$$\frac{[RONO_2]_i}{[RONO_2]_j} = \frac{\beta_i}{\beta_j}. \quad (10)$$

The left hand side of equation (10) is termed the measured ratio, m_{meas}, because it can be quantified by atmospheric measurements. The right hand side is the predicted ratio, $m_{pred} = \beta_i/\beta_j$, which is based on the branching ratios α_1 and α_2. The C_5 alkyl nitrates 2-$PeONO_2$ and 3-$PeONO_2$ both originate from *n*-pentane, and the slope of 3-$PeONO_2$ vs. 2-$PeONO_2$ is expected to equal $\beta_{3\text{-}PeONO2}/\beta_{2\text{-}PeONO2}$ for freshly polluted air masses. By contrast, equation (10) does not apply for alkyl nitrates $<C_4$ because they are formed from the decomposition of other, larger alkoxy radicals in addition to their parent hydrocarbons [*Flocke et al.*, 1998; *Roberts et al.*, 1998].

4. Results and Discussion

[17] This paper focuses on three aspects of photochemical alkyl nitrate production and evolution. In all three cases, TRACE-P alkyl nitrate measurements are compared with predictions based on laboratory kinetic studies. First, the photochemical production of 3-$PeONO_2$ and 2-$PeONO_2$ from *n*-pentane in relatively fresh air masses (where photochemical losses are likely negligible compared to production) are used to assess laboratory predictions of C_5 alkyl nitrate production. Second, $RONO_2$/RH ratios are used to quantitatively investigate photochemical processing within air masses sampled during TRACE-P. Third, $RONO_2$/RH ratios are used to detect additional sources of alkyl nitrate precursors in Asian outflow. The two young, polluted plumes used in the first and second investigations are described below, following an overview of the alkyl nitrates sampled during TRACE-P.

4.1. Overview of TRACE-P Alkyl Nitrate Measurements

[18] Of the 5493 whole air samples collected aboard the NASA DC-8 and P-3B research aircraft during TRACE-P, the percentage of measurements in which alkyl nitrates were detectable exceeded 99% for all reported alkyl nitrates $\leq C_4$, 97% for 2-$PeONO_2$, and 84% for 3-$PeONO_2$. The mixing ratios of the C_2–C_5 alkyl nitrates decreased with increasing altitude (Table 3), consistent with their surface sources and their short atmospheric lifetimes relative to the vertical tropospheric mixing time of ~1 month. The maximum abundance of 2-$PrONO_2$ and 2-$BuONO_2$ indicates the importance of photochemical alkyl nitrate production during TRACE-P.

[19] The TRACE-P alkyl nitrate mixing ratios can be compared to studies in urban continental, rural continental, and marine environments (Table 4). For example, in Karachi, Pakistan during winter, *Barletta et al.* [2002] measured mean ground-level C_2–C_4 mixing ratios that are 2–3 times larger than the mean values reported between 0 and 2 km during TRACE-P. In Athens, Greece during summer, *Glavas and Moschonas* [2002] measured mean 2-$PeONO_2$ and 3-$PeONO_2$ mixing ratios that are 5–9 times higher than the mean mixing ratios sampled between 0–2 km during TRACE-P and comparable to the maximum TRACE-P mixing ratios measured between 0 and 2 km. In rural Alabama during summer, *Bertman et al.* [1995] measured mean alkyl nitrate mixing ratios that are

Table 3. Alkyl Nitrate Mixing Ratio Statistics (pptv) for All DC-8 and P-3B Flights of the TRACE-P Mission[a]

	Minimum			Maximum			Median			Mean			Standard Deviation		
Compound	0–2 km	2–7 km	7–12 km	0–2 km	2–7 km	7–12 km	0–2 km	2–7 km	7–12 km	0–2 km	2–7 km	7–12 km	0–2 km	2–7 km	7–12 km
$EtONO_2$	0.80	0.12	0.05	19.3	7.7	8.0	4.1	2.1	1.4	4.2	2.3	1.6	1.8	1.2	0.9
1-$PrONO_2$	0.14	0.01	LOD	10.6	3.6	3.3	1.6	0.5	1.4	1.7	0.6	0.3	1.0	0.6	0.4
2-$PrONO_2$	0.72	0.06	0.02	56.4	22.7	19.7	10.7	3.4	1.3	11.1	4.4	2.1	6.4	3.5	2.3
2-$BuONO_2$	0.25	0.01	0.01	67.1	29.3	22.9	11.9	2.0	0.3	13.0	3.7	1.1	9.0	4.3	2.3
2-$PeONO_2$	0.03	LOD	LOD	30.1	10.0	7.3	3.4	0.5	0.1	4.1	1.0	0.3	3.1	1.3	0.6
3-$PeONO_2$	LOD	LOD	LOD	20.0	7.8	5.7	2.7	0.3	LOD	3.2	0.7	0.2	2.5	1.1	0.5

[a]A total of 5493 samples were collected at altitudes between 150 m and 12 km, mainly over the western and central Pacific. At low altitudes including the marine boundary layer (0–2 km), the number of samples (n) was 1732; in the lower free troposphere (2–7 km) n = 2835; in the upper troposphere and lower stratosphere (7–12 km) n = 926. LOD = limit of detection.

similar to those measured between 0 and 2 km during TRACE-P, with the exception of $EtONO_2$, which was three times higher in the Alabama study. At the remote Mauna Loa Observatory in Hawaii during late spring, *Elliot et al.* [1992] measured upslope mixing ratios that are generally much smaller than those observed during TRACE-P. *Stroud et al.* [2001] measured airborne alkyl nitrate mixing ratios over the northeastern plains of Colorado during summer, between altitudes of 0 and 7 km. Their mean alkyl nitrate mixing ratios lie in between the TRACE-P means for 0–2 km and 2–7 km, although the results are not statistically different. Overall, individual alkyl nitrate measurements during the TRACE-P mission covered the range from clean remote air to polluted continental air. The mean TRACE-P measurements were of similar magnitude to alkyl nitrate mixing ratios in rural continental air from the United States.

4.2. Shanghai Plume

[20] A fresh, well-defined plume was encountered at an altitude of 330 m on 21 March 2001 from 1335–1355 local time (0435–0455 UTC) during DC-8 Flight 13 (Figure 1). This was a local flight deployed from Yokota Air Force Base and flown over the Yellow and East China Seas. The plume was characterized by high levels of short-lived compounds such as ethene (lifetime $\sim$ 1–2 days) and propene (lifetime $\sim$ 8–12 hours) (680–3050 pptv and 5–110 pptv, respectively). However, the very short-lived hydrocarbon *trans*-2-butene (lifetime $\sim$ 4 hours) did not exceed its detection limit during the plume encounter. The plume contained the highest pentyl nitrate levels of the mission, with mixing ratios up to 30 pptv (2-$PeONO_2$) and 20 pptv (3-$PeONO_2$) (Figure 2a). These mixing ratios are comparable to mean mixing ratios measured in the city of Athens during summer [*Glavas and Moschonas*, 2002]. Based on the observed mixing ratios of compounds with major anthropogenic sources, such as carbon monoxide (CO) and the industrial tracer tetrachloroethene (C_2Cl_4), the Shanghai plume was the most polluted air mass sampled during the TRACE-P mission. During the plume encounter, C_2Cl_4 mixing ratios exceeded 120 pptv, compared with a median C_2Cl_4 mixing ratio of 5 pptv during the remainder of the flight.

[21] Five-day backward trajectories provided by Florida State University (FSU) suggest that the plume had encountered the city of Shanghai on the Asian coast roughly 18 hours prior to sampling. The high levels of short-lived alkenes suggest that the Shanghai plume was relatively fresh and is a good candidate for investigating the photochemical production of C_5 alkyl nitrates. The requirement to consider only chemical terms in applying equation (10) is satisfied because the marine source of C_5 alkyl nitrates is expected to be small (section 1). In addition, dilution is presumed to act equally on 2-$PeONO_2$ and 3-$PeONO_2$ because of their similar lifetimes (Table 2).

4.3. Seoul Plume

[22] The second-highest pentyl nitrate mixing ratios during TRACE-P were encountered during a spiral into the marine boundary layer aboard P-3B Flight 19, a local flight deployed from Yokota Air Force Base and flown over the Sea of Japan (Figure 1). The spiral occurred on 3 April 2001 between 1310 and 1320 local time (0410–0420 UTC). Mixing ratios as high as 16 pptv (2-$PeONO_2$) and 12 pptv (3-$PeONO_2$) were measured at altitudes below 900 m (Figure 2b). Five-day backward trajectories show that the air mass had traveled over Beijing roughly 1.5 days prior to sampling, then had been advected over Seoul 0.5–1 day prior to sampling. As with the Shanghai plume, mixing ratios of the very short-lived hydrocarbon *trans*-2-butene did not exceed its detection limit during the plume encounter, but elevated mixing ratios of propene (5–25 pptv) and ethene (140–790 pptv) were again detected.

[23] To investigate possible influence of Beijing air (which would contribute relatively aged components) on

Table 4. Mean Alkyl Nitrate Mixing Ratios (pptv) Measured at Selected Urban, Rural, and Marine Locations[a]

Compound	Urban Karachi Mixing Ratio[b]	Urban Athens Mixing Ratio[c]	Rural Alabama Mixing Ratio[d]	Mauna Loa Mixing Ratio[e]	STERAO Mixing Ratio[f]
$EtONO_2$	15.5 ± 4.6	n/a	12	n/a	2.8 ± 1.7
1-$PrONO_2$	5.0 ± 1.6	n/a	2	0.67 ± 0.25	1.4 ± 1.0
2-$PrONO_2$	21.0 ± 7.6	n/a	13	1.91 ± 0.84	8.7 ± 6.6
2-$BuONO_2$	25.1 ± 12.8	n/a	14	1.55 ± 0.81	5.9 ± 6.4
2-$PeONO_2$	n/a	35	7	0.37 ± 0.20	n/a
3-$PeONO_2$	n/a	16	4	0.25 ± 0.17	1.3 ± 1.3

[a]All air samples were collected at ground level with the exception of the Stratospheric Tropospheric Exchange: Radiation, Aerosols, and Ozone (STERAO) measurements, which were airborne samples collected over the northeastern plains of Colorado. Error bars represent 1 standard deviation. n/a = not available.
[b]*Barletta et al.* [2002].
[c]*Glavas and Moschonas* [2001].
[d]*Bertman et al.* [1995].
[e]*Atlas et al.* [1992].
[f]*Stroud et al.* [2001].

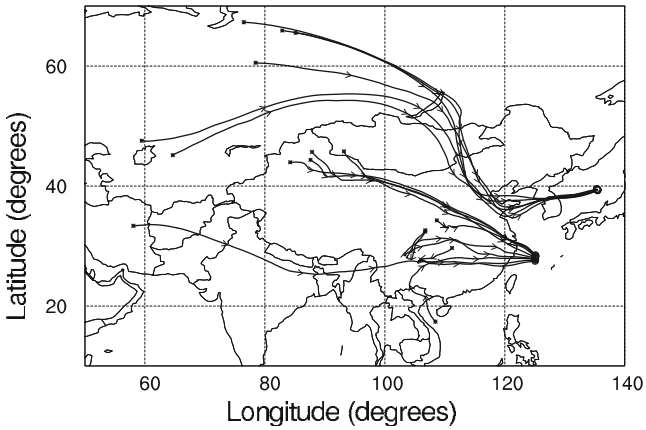

Figure 1. Sampling locations of the Shanghai plume (28.8–30.3°N; 125.1–125.2°E) and the Seoul plume (39.2–39.5°N; 135.3–135.4°E), together with their respective 5-day backward trajectories.

the sampled air mass, chemical tracers distinctive of emissions from China (halon 1211 or H-1211, and methyl chloride or CH_3Cl [*Blake et al.*, 2001]) and Japan/Korea (methyl bromide or CH_3Br) were examined. The plume showed a 150% increase in CH_3Br mixing ratios relative to the rest of the flight, with only minor increases in H-1211 (7%) and CH_3Cl (8%). By contrast, the Shanghai plume showed large enhancements of both H-1211 (225%) and CH_3Cl (115%). These results suggest that the plume encountered during P-3B Flight 19 was strongly influenced by pollution from Seoul, with little influence from Beijing pollution sources further upwind. The backward trajectories transit over Beijing around midnight local time, at altitudes above 700 hPa (2.5 km). We believe that the Seoul plume shows little influence from Beijing because Beijing's pollution was contained within a compressed nighttime boundary layer, and the trajectories passed over Beijing at an altitude above the main pollution layer. The freshness of the Seoul emissions and the large pentyl nitrate mixing ratios suggest that the Seoul plume is also a good candidate for investigating the photochemical production of C_5 alkyl nitrates. Detailed evidence that supports using the Shanghai and Seoul plumes in this investigation is given in section 4.5.

4.4. Photochemical Production of C_5 Alkyl Nitrates

[24] The measured slopes of 3-$PeONO_2$ vs. 2-$PeONO_2$ during the Shanghai and Seoul plume encounters were 0.60 ± 0.01 pptv/pptv (r^2 = 0.998) and 0.65 ± 0.02 pptv/pptv (r^2 = 0.996), respectively (Figure 2a–2b). That is, for every 100 molecules of 2-$PeONO_2$ that were formed from the oxidation of *n*-pentane, 60–65 molecules of 3-$PeONO_2$ were produced. The slopes from the Shanghai and Seoul plumes show excellent agreement with a slope m_{meas} = 0.63 ± 0.06 pptv/pptv from a ground-based field study in Germany [*Flocke et al.*, 1998]. They also lie within the uncertainty range of m_{meas} = 0.68 ± 0.09 pptv/pptv based on upslope measurements at the Mauna Loa Observatory [*Atlas et al.*, 1992]. However, the Mauna Loa air samples are likely more aged than the Shanghai and Seoul plumes and as a result are not expected to be good candidates for comparison with m_{pred} (see section 4.5.1).

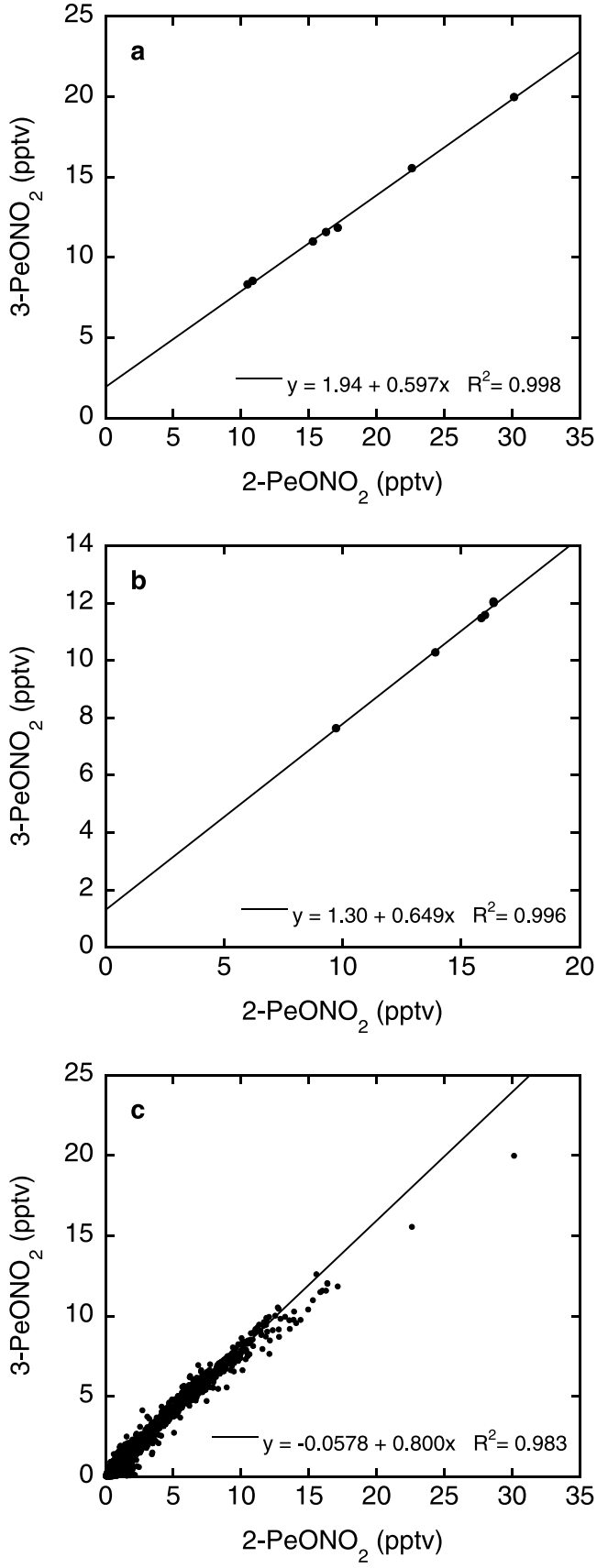

Figure 2. Measured mixing ratios of 3-$PeONO_2$ versus 2-$PeONO_2$ during TRACE-P. (a) Shanghai plume; (b) Seoul plume; (c) all TRACE-P DC-8 and P-3B flights.

Table 5. Branching Ratios Leading to the Formation of Daughter Alkyl Nitrates From Parent Hydrocarbons (See Equations (1) and (3b))[a]

		α_1[b]		α_2[c]		β[d]	
Parent RH	Daughter $RONO_2$	1987	1995	1987	2001	1987, 1987	1995, 1901
Ethane	$EtONO_2$	1	1	<0.014	0.006*	<0.014	0.006*
Propane	1-$PrONO_2$	0.307	0.264	0.020	n/a	0.006	0.005*
Propane	2-$PrONO_2$	0.693	0.736	0.042	0.039	0.029	0.029
n-Butane	2-$BuONO_2$	0.853	0.872	0.090	0.084	0.077	0.073
n-Pentane	2-$PeONO_2$	0.550	0.568	0.129	0.106	0.071	0.060
n-Pentane	3-$PeONO_2$	0.356	0.349	0.131	0.126	0.047	0.044

[a]Here α_1 is the formation yield of a parent alkyl radical from the reaction of a parent hydrocarbon with OH; α_2 is the formation yield of a daughter alkyl nitrate from the reaction of a parent alkyl peroxy radical with NO; β is $\alpha_1\alpha_2$.

[b]Here α_1 was calculated using rate constants for the abstraction of hydrogen atoms from C_3-C_5 *n*-alkanes. These rate constants were determined using the group rate constants and group substituent factors derived by *Atkinson* [1987] and revised by *Kwok and Atkinson* [1995].

[c]Here α_2 values are from *Atkinson et al.* [1987] and *Arey et al.* [2001].

[d]Here β was calculated using both older and newly published values of α_1 and α_2. For example, "1987, 1987" pairs α_1 values from *Atkinson* [1987] with α_2 from *Atkinson et al.* [1987]. An asterisk denotes that new α_2 branching ratios are not available from *Arey et al.* [2001] for $EtONO_2$ and 1-$PrONO_2$. For $EtONO_2$, 0.006 is the α_2 branching ratio reported by *Ranschaert et al.* [2000] at 298 K. For 1-$PrONO_2$, β has been calculated by pairing newer α_1 values from *Kwok and Atkinson* [1995] with older α_2 values from *Atkinson et al.* [1987].

[25] The measured slopes can be compared with the predicted slope $m_{pred} = \beta_i/\beta_j$, which is based on the branching ratios α_1 and α_2 (Table 5). Here, m_{pred} was calculated using both old and newly published values of α_1 and α_2 in order to investigate the magnitude by which m_{pred} is affected by the new branching ratios (Table 6). The branching ratio α_1 was calculated from the structure-activity relationships described by *Atkinson* [1987], using the parameters derived by *Atkinson* [1987] and updated by *Kwok and Atkinson* [1995] (Table 1). The reader is referred to *Finlayson-Pitts and Pitts* [2000] for a detailed sample calculation. For the alkyl nitrates listed in Table 5, the new structure-activity parameters caused the largest change for the primary alkyl nitrates: α_1 decreased by 14% for 1-$PrONO_2$, whereas α_1 increased by 2–6% for secondary $RONO_2$, and decreased by 2% for 3-$PeONO_2$.

[26] *Arey et al.* [2001] present new values of alkyl nitrate formation yields from parent RO_2 molecules (α_2) and from parent RH molecules ($\alpha_1\alpha_2$) for selected C_5-C_8 alkyl nitrates. The C_5 values cited by *Arey et al.* [2001] are based on work by *Atkinson et al.* [1995]. For hexyl, heptyl, and octyl nitrates, the sum of isomeric alkyl nitrate yields from a given parent *n*-alkane are about 32, 39, and 29% lower, respectively, than data previously reported from the same laboratory by *Atkinson et al.* [1982]. Although the new total pentyl nitrates yields are about 10% lower than the earlier data, the results are not statistically different to within the stated uncertainties. *Arey et al.* [2001] suspect that wall losses (especially during calibration) may have contributed to the higher yields in the earlier study, in contrast to the new studies in which wall losses during calibration were verified to be minor or negligible.

[27] The predicted slope of 3-$PeONO_2$ versus 2-$PeONO_2$ ranges from 0.63 to 0.66 when α_1 values from *Atkinson* [1987] and *Kwok and Atkinson* [1995] are paired with older α_2 values from *Atkinson et al.* [1987] (Table 6). *Flocke et al.* [1998] found that within their error limits, their reported value of $m_{meas} = 0.63 \pm 0.06$ agreed well with $m_{pred} = 0.66$ based on older α_1 and α_2 values. When newer α_2 values are used, m_{pred} increases by 16% to 0.73–0.77. The increase is caused by the larger decrease of α_2 for 2-$PeONO_2$ relative to 3-$PeONO_2$ (Table 5). Pairing the newer values of α_1 and α_2 gives the lower result of $m_{pred} = 0.73$. The uncertainty in $m_{pred} = 0.73$ can be determined from the uncertainties in the formation yields ($\alpha_1\alpha_2$) of 3-$PeONO_2$ (0.044 ± 0.006) and 2-$PeONO_2$ (0.060 ± 0.010) from *n*-pentane [*Arey et al.*, 2001]. The uncertainty in m_{pred}($= 0.044 \div 0.060$) is given by $\sqrt{(0.044)^2(0.006)^2 + (0.060)^2(0.010)^2} = 0.08$.

[28] The slope of 3-$PeONO_2$ versus 2-$PeONO_2$ during Shanghai plume encounter is significantly smaller than the newest predicted slope from laboratory kinetic studies, whereas the slope measured during the Seoul plume encounter does not significantly differ from $m_{pred} = 0.73 \pm 0.08$ (Table 6). Overall, the ratio between the production rates of 3-$PeONO_2$ and 2-$PeONO_2$ from *n*-pentane measured during this study ($m_{meas} = 0.60-0.65$) shows better agreement with predicted slopes using older values of α_2 ($m_{pred} = 0.63-0.66$) than with predicted pentyl nitrate production rates using the most recent values of α_1 and α_2 ($m_{pred} = 0.73 \pm 0.08$). These comparisons suggest that the ratio between the production rates of 3-$PeONO_2$ and 2-$PeONO_2$ from *n*-pentane likely lies near the lower limit of the reported uncertainty range for the most recent value of $m_{pred} = 0.73 \pm 0.08$.

Table 6. Measured and Predicted Slopes (m_{meas} and m_{pred}, Respectively) for 3-$PeONO_2$ Versus 2-$PeONO_2$[a]

m_{meas}	Reference	m_{pred}	α_1 Reference	α_2 Reference
0.63 ± 0.06	*Flocke et al.* [1998]	0.66	*Atkinson* [1987]	*Atkinson et al.* [1987]
0.60 ± 0.01	Shanghai plume	0.63	*Kwok and Atkinson* [1995]	*Atkinson et al.* [1987]
0.65 ± 0.02	Seoul plume	0.77	*Atkinson* [1987]	*Arey et al.* [2001]
		0.73 ± 0.08	*Kwok and Atkinson* [1995]	*Arey et al.* [2001]

[a]The measured slopes from TRACE-P were calculated for the young, highly polluted Shanghai and Seoul plumes.

4.5. Evolution of 3-$PeONO_2$/2-$PeONO_2$

[29] In this section we quantitatively show why young air masses such as the Shanghai and Seoul plumes are the best candidates of the TRACE-P data set for comparing the photochemical production of C_5 alkyl nitrates with laboratory predictions. The evolution of 3-$PeONO_2$/2-$PeONO_2$ within the Shanghai plume is used as an example. The sensitivity of the modeled 3-$PeONO_2$/2-$PeONO_2$ ratio to the applied initial conditions is also discussed.

4.5.1. Shanghai Plume Evolution

[30] To predict the time evolution of 3-$PeONO_2$/2-$PeONO_2$ within the Shanghai plume, equation (9) was rearranged to solve for the daughter pentyl nitrate:

$$[\mathrm{PeONO_2}] = [\text{n pentane}]\frac{bk_A}{(k_B - k_A)}\left(1 - e^{(k_A - k_B)t}\right). \quad (11)$$

We note that dilution is neglected in this equation (see section 4.5.2). Equation (11) was then solved for both 3-$PeONO_2$ and 2-$PeONO_2$ under conditions appropriate for the Shanghai plume, from $t = 0$ to $t = 30$ days. The newest values of α_1 and α_2 from the literature were used to calculate β (Table 5). A diurnally averaged surface-level OH concentration of $[8.8 \pm 4.7] \times 10^5$ molec cm^{-3} was used in calculating k_A and k_B. This OH value was determined for TRACE-P conditions (35–41°N, 0–1 km) using a model previously described by *Crawford et al.* [1999]. Diurnal *J*-values are also required to determine k_B, and they were calculated assuming a clear sky using absorption cross sections reported by *Roberts and Fajer* [1989] and conditions appropriate for TRACE-P (1 April, 40°N, ozone column = 350 Dobson Units; Table 2), also using the model described by *Crawford et al.* [1999]. The reader is referred to *Clemitshaw et al.* [1997] and *Talukdar et al.* [1997] for a comparison of alkyl nitrate ultraviolet absorption cross-sections obtained from various laboratory studies since the late 1980s.

[31] The time evolution of *n*-pentane is also required to solve equation (11) and was determined as follows. First, the initial concentration of *n*-pentane, $[n\text{-pentane}]_0$, was calculated using:

$$[\text{n pentane}]_0 = \frac{[\text{n pentane}]}{e^{-k_A t}}. \quad (12)$$

During the Shanghai plume encounter, the average mixing ratio of *n*-pentane was 365 ± 202 pptv (1 pptv = 2.46×10^7 molec cm^{-3} at the Earth's surface). The 18-hour transit time of the Shanghai plume was used to approximate the elapsed time *t* (the age of the Shanghai plume is examined in detail in section 4.5.2). The diurnally averaged OH concentration of 8.8×10^5 molec cm^{-3} gives $k_A = 3.5 \times 10^{-6}$ s^{-1}. Solving equation (12) under these conditions gives $[n\text{-pentane}]_0 \sim 460$ pptv (1.1×10^{10} molec cm^{-3}). Equation (12) was next rearranged to its more familiar form:

$$[\text{n pentane}] = [\text{n pentane}]_0 e^{-k_A t} \quad (13)$$

allowing the depletion of *n*-pentane to be modeled from $t = 0$ to $t = 30$ days (Figure 3a). The calculated *n*-pentane values were then used to solve equation (11) for 2-$PeONO_2$ and 3-$PeONO_2$. We note that once a value of OH has been selected, the only two values that change with time in equation (11) are time itself, *t*, and [*n*-pentane], which decreases with time. The way in which [*n*-pentane] and *t* interact with each other determines the shape of the 2-$PeONO_2$ and 3-$PeONO_2$ time evolution curves.

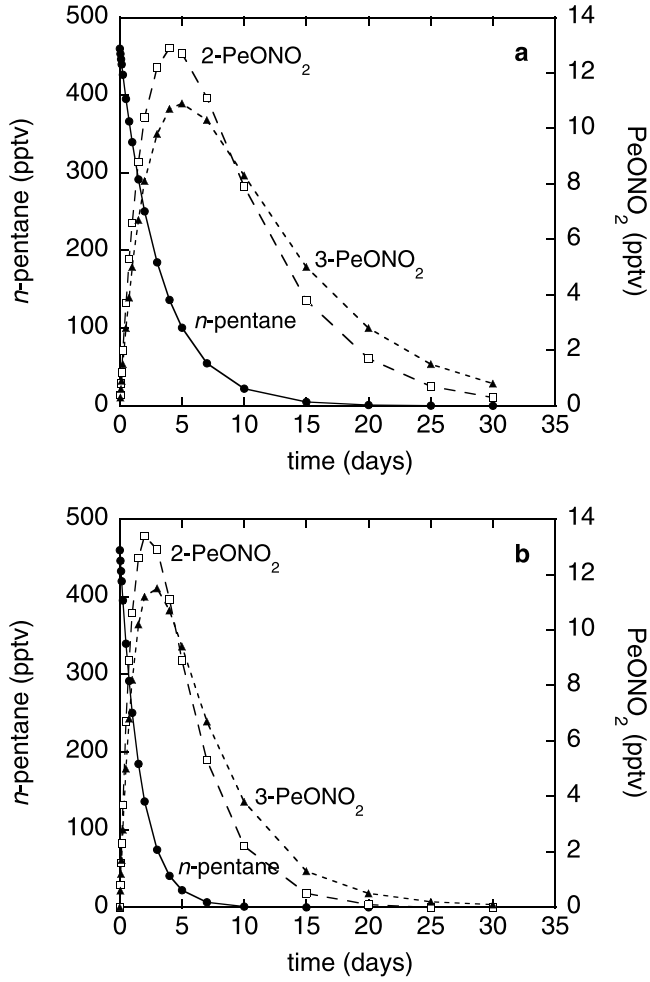

Figure 3. Modeled time evolution of *n*-pentane, 2-$PeONO_2$ and 3-$PeONO_2$ under selected applied conditions (see text). (a) [OH] = 8.8×10^5 molec cm^{-3}; (b) [OH] = 17.6×10^5 molec cm^{-3}.

[32] 2-Pentyl nitrate peaks both earlier and at a higher value than 3-$PeONO_2$ (Figure 3a). 2-Pentyl nitrate peaks at a higher value than 3-$PeONO_2$ because the combined branching ratio β for the photochemical formation of 2-$PeONO_2$ is larger than that for 3-$PeONO_2$ (Table 5). 2-Pentyl nitrate peaks earlier than 3-$PeONO_2$ because OH reacts more readily with 2-$PeONO_2$ than with 3-$PeONO_2$, whereas the surface-level photolysis rate constants are similar for 2- and 3-$PeONO_2$ (Table 2). Together, the photochemical production and destruction of the pentyl nitrates combine such that the ratio of 3-$PeONO_2$/2-$PeONO_2$ increases with time from its initial predicted value of 0.73 at $t = 0$ (Figure 4).

[33] This modeled increase in the ratio of 3-$PeONO_2$/2-$PeONO_2$ with photochemical processing is consistent with measured 3-$PeONO_2$/2-$PeONO_2$ ratios during TRACE-P.

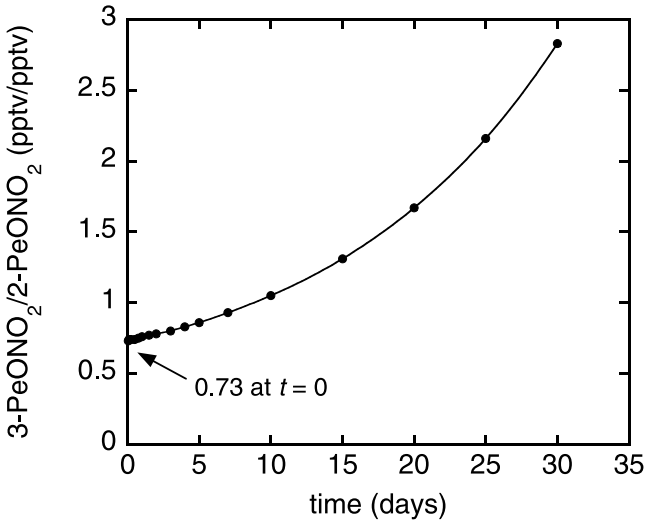

Figure 4. Modeled time evolution of 3-$PeONO_2$/2-$PeONO_2$ using [*n*-pentane]$_0$ = 460 pptv, [OH] = 8.8 × 10^5 molec cm^{-3}, and kinetic parameters from Table 1.

The slopes of 3-$PeONO_2$/2-$PeONO_2$ during the Shanghai and Seoul plume encounters (0.60 ± 0.01 and 0.65 ± 0.02, respectively) are lower than a measured slope of 0.80 when data points from all the TRACE-P flights (which comprise more aged air masses) are included (Figure 2a–2c). In Figure 2c the elevated mixing ratios in the top right quadrant of the graph represent the young Shanghai and Seoul plumes, and they lie below the fitted line.

[34] The key point to take from Figure 4 is that when selecting field data from which to calculate m_{meas} for comparison to m_{pred}, younger air samples are more appropriate because they are expected to better approximate m_{pred}. Under the conditions used to generate Figure 4, the ratio of 3-$PeONO_2$/2-$PeONO_2$ is predicted to increase 5% after one day of processing and 11% after two days. For the <1 day old Shanghai plume (section 4.5.2), the measured slope of 0.60 is expected to be within 5% of its initial value at $t = 0$. As a result young, polluted air masses such as the Shanghai and Seoul plumes are considered to be the best candidates of the TRACE-P field data set for comparison with predicted slopes from laboratory kinetic studies. Because the slope of 3-$PeONO_2$/2-$PeONO_2$ is predicted to increase exponentially with time, we suggest that air mass age of less than one or two days is a more useful criterion for applying equation (10) than our earlier, qualitative assumption that photochemical loss is negligible compared to production.

4.5.2. Sensitivity to Initial Conditions

[35] Based on the estimated initial *n*-pentane mixing ratio of 460 pptv for the Shanghai plume, 2-$PeONO_2$ and 3-$PeONO_2$ are predicted to peak at values of 13 pptv and 11 pptv, respectively (Figure 3a). By comparison, the average mixing ratios of 2-$PeONO_2$ and 3-$PeONO_2$ measured in the Shanghai plume were 17.5 ± 6.9 pptv and 12.4 ± 4.1 pptv, respectively. That is, the modeled peak mixing ratios are similar to values measured within the Shanghai plume, to within the natural variability of the measurements. However, when making these comparisons it is important to recognize that the $RONO_2$ concentrations measured in the Shanghai plume may not be the peak values. Instead, the measured mixing ratios could lie before or after the plume's peak values.

[36] Direct comparison between the measured and modeled results is also impeded because an assumption in the application of equation (11) is that the initial concentration of the alkyl nitrate is zero, whereas in reality alkyl nitrate production would have begun (1) in Shanghai before the ventilation of the plume from the city and (2) possibly further upwind in air that was advected through Shanghai. In the latter case, influence from upwind air appears to be unlikely. Because ethyne is relatively short-lived (lifetime ~2–3 weeks) compared to CO (lifetime ~ 2 months), the ratio of ethyne/CO can be used to assess the amount of atmospheric processing (photochemical reaction + dynamic mixing) within an air mass [*Smyth et al.*, 1996]. A ratio of 4–5 pptv/ppbv indicates unprocessed air; a ratio of 1–2 represents processed air; and a ratio of less than 1 indicates very processed air (E. Browell, NASA-Langley, personal communication, 2002). The median ethyne/CO ratio during the Shanghai plume encounter was 6.3 pptv/ppbv, with individual values ranging from 5.0 to 9.4 pptv/ppbv (the CO measurements were made by Glen Sachse, NASA-Langley). These results show that the Shanghai plume samples were unprocessed and were not significantly impacted by more aged components from further upwind.

[37] The extent of photochemical processing within Shanghai depends in part on the city's "ventilation time," the time required for an emitted pollutant to be transported downwind of the city. *Streets et al.* [1999] report on air quality in Shanghai, and based on their work the most frequent wind speed class in Shanghai during the spring season is 3–8 m s^{-1}, with an average of 5.5 m s^{-1} or roughly 20 km hr^{-1} (J.-H. Woo, University of Iowa, personal communication, 2002). Surface winds measured in Shanghai the day before sampling (20 March 2001) were higher than average, at roughly 10 m s^{-1}. Pollutants that are emitted from central Shanghai need to travel roughly 50 km downwind to be ventilated from the city. Assuming a relatively constant wind direction, pollutants emitted in central Shanghai were likely transported downwind of the city in less than 2 hours on 20 March, and the age of the Shanghai plume is expected to be only a few hours older than its 18-hour transit time to the sampling location over the Pacific Ocean. The photochemical production of alkyl nitrates within Shanghai is expected to remain low as a result of Shanghai's multiple daily ventilations. However, a background alkyl nitrate concentration of even a few pptv in Shanghai violates the assumption of zero initial alkyl nitrate concentration in the application of equation (11), given that a few pptv represents a reasonable fraction of the mean 2-$PeONO_2$ and 3-$PeONO_2$ mixing ratios measured within the Shanghai plume (17.5 ± 6.9 pptv and 12.4 ± 4.1 pptv, respectively).

[38] Dilution competes with chemistry on all timescales, and its effect on the Shanghai plume during its 18-hour transit over the ocean must also be considered. In previous studies the ratios of various hydrocarbons have been shown to change as a function of both photochemistry and atmospheric mixing [*McKeen and Liu*, 1993; *McKeen et al.*, 1996]. In the comparison between 2-$PeONO_2$ and 3-$PeONO_2$, dilution is presumed have a similar effect on

both species because of their comparable lifetimes (Table 2), and the effect of dilution is expected to largely cancel in the ratio of 3-$PeONO_2$/2-$PeONO_2$.

[39] Finally, we consider the OH concentration that was applied in equation (11). Based on [OH] = 8.8×10^5 molec cm^{-3} (section 4.5.1), equation (11) predicts maximum 2-$PeONO_2$ and 3-$PeONO_2$ mixing ratios after 4 and 5 days, respectively. When the concentration of OH used to calculate k_A and k_B is doubled, the pentyl nitrate lifetimes with respect to OH are halved, and the pentyl nitrate concentrations peak two days earlier (Figure 3b). That is, the time at which the pentyl nitrate peaks are predicted to occur is highly sensitive to the amount of OH that is used to solve equation (11).

[40] The measured OH mixing ratio in the Shanghai plume was 0.12–0.19 pptv ($3.0–4.7 \times 10^6$ molec cm^{-3}) (H. Harder, Pennsylvania State University, personal communication, 2002). In the Shanghai plume's estimated 18 hour backward trajectory we estimate that roughly 7 hours (from 0630 to 1330 local time) were spent in daylight. Although OH exhibits a strong diurnal variation, its average mixing ratio was fairly constant between 0930 and 1330 during low-altitude flight legs of Flight 13 (0.16 ± 0.02 pptv; http://www-gte.larc.nasa.gov/trace/gte_mrg1.htm# TRACE-P), suggesting a widespread area of high OH concentration over the East China Sea on the day of sampling. If we apply 0.16 pptv from 0930 to 1330, and an estimated average OH concentration of 0.08 pptv from 0630 to 0930 (from 0 pptv at sunrise to 0.16 pptv at 0930), then the average OH concentration during the 18 hour plume travel time was 1.2×10^6 molec cm^{-3} (1 pptv = 2.47×10^7 molec cm^3 at the Earth's surface). This is 35% higher than the applied value of 8.8×10^5 molec cm^{-3}. The plume likely spent a couple hours in Shanghai before being ventilated from the city at roughly 1930 local time on 20 March, and additional reaction with OH is expected to have occurred within Shanghai that late afternoon/early evening. Despite the uncertainties in these calculations (such as variations in daytime OH levels and the exact amount of time spent in Shanghai before ventilation), the average OH level in the Shanghai plume's history was likely larger than the OH value that was applied in the model.

[41] In summary, the modeled pentyl nitrate mixing ratios are highly sensitive to the amount of OH that is assumed in the history of the air mass. In the case of the Shanghai plume, a direct comparison between the measured and modeled pentyl nitrate mixing ratios was not possible because background pentyl nitrate mixing ratios within Shanghai were not quantified, such that the condition of zero initial alkyl nitrate concentration could not be verified. In addition, it was not known whether the Shanghai plume was sampled at/near the peak pentyl nitrate concentrations. These unknowns precluded using the Shanghai plume measurements to validate the time and magnitude of the pentyl nitrate peaks that were predicted using equation (11).

4.6. Evolution of $C_2–C_5$ Alkyl Nitrates

[42] In photochemical alkyl nitrate evolution, the ratio of a daughter alkyl nitrate to its parent hydrocarbon increases as an air mass ages because the daughter alkyl nitrate is produced at the expense of its parent hydrocarbon. Here $RONO_2$/RH ratios are calculated for the measured $C_2–C_5$ alkyl nitrates and compared to modeled curves based on laboratory kinetic data.

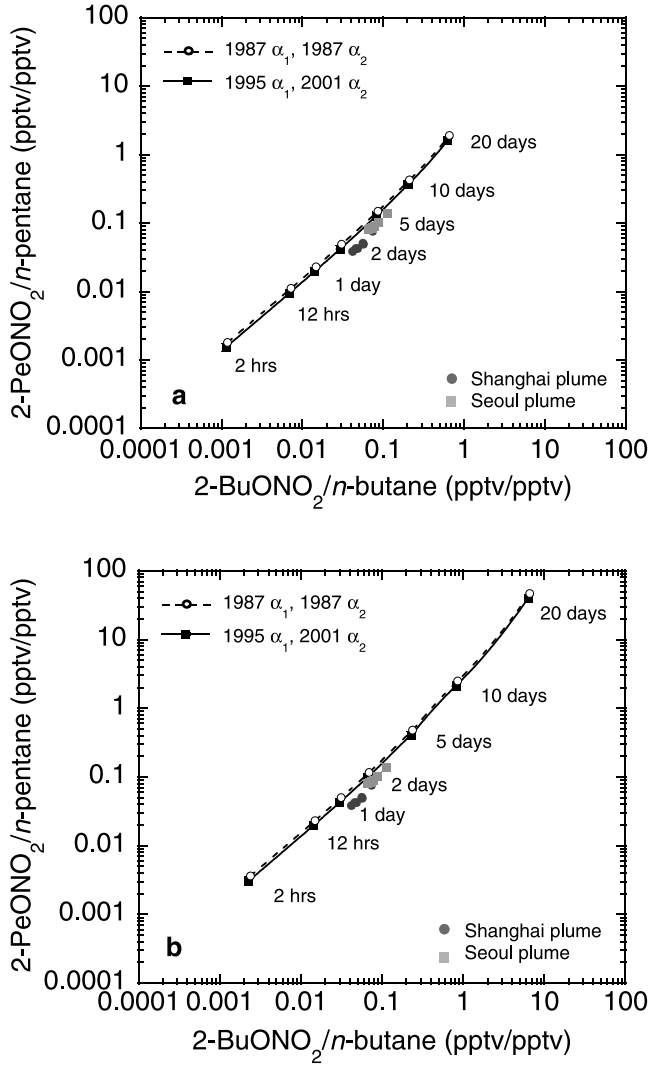

Figure 5. Modeled time evolution of 2-$PeONO_2$/*n*-pentane versus 2-$BuONO_2$/*n*-butane for surface-level conditions (see text). (a) [OH] = 8.8×10^5 molec cm^{-3}; (b) [OH] = 17.6×10^5 molec cm^{-3}. The dashed and solid curves show results that were calculated using older and newer branching ratios from the literature, respectively.

4.6.1. Photochemical Processing Times

[43] Before attempting to quantify the amount of photochemical processing within an air mass using $RONO_2$/RH ratios, dilution needs to be considered, in addition to the sensitivity of the modeled evolution curves to the kinetic data required to solve equation (9) (k_1, k_4, α_1, α_2, [OH] and J). In the latter case, the modeled ratios of 2-$PeONO_2$/*n*-pentane vs. 2-$BuONO_2$/*n*-butane are used as an example. The modeled slope is found to vary only slightly depending on whether older or newer branching ratios from the literature are used (Figure 5a). Although the position of the line is quite insensitive to changes in the OH concentration, the times associated with a particular position on the line are seen to change with the OH concentration (Figure 5b).

[44] Whereas recent alkyl nitrate field studies have been performed at ground-level [*Bertman et al.*, 1995; *Flocke et al.*, 1998; *Roberts et al.*, 1998], the TRACE-P data set includes samples collected throughout the troposphere from 150 m to 12 km. *Stroud et al.* [2001] also measured alkyl nitrate mixing ratios in the lower and middle troposphere (0–7 km). At present it is not possible to fully quantify the effect of altitude on alkyl nitrate evolution because k_4 values are not available for $RONO_2$ + OH reaction at temperatures colder than 290 K [*Atkinson et al.*, 1997]. By comparison, an average temperature of 230 ± 5 K was measured in the upper troposphere (9.5–10.5 km) during TRACE-P http://www-gte.larc.nasa.gov/trace/gte_mrg1.htm#TRACE-P). However, we can briefly consider the effect of altitude on the remaining kinetic parameters used to solve equation (9). The hydroxyl radical concentration and k_1 both decrease with increasing altitude (decreasing temperature), leading to slower alkyl nitrate production (Table 2). Although the lower [OH] values at higher altitude also lead to slower alkyl nitrate destruction by OH, alkyl nitrate *J*-values increase with altitude (section 3.2). In this study *J*-values were calculated at 10 km under TRACE-P conditions, although the absorption cross sections were applied assuming no temperature dependence (Table 2). Because including temperature-dependent cross sections causes J_{RONO2} to increase more slowly with increasing altitude [*Talukdar et al.*, 1997], the *J*-values calculated at 10 km are expected to be too large and the amount of alkyl nitrate destruction by photolysis at 10 km is likely overestimated. As stated above, temperature-dependent k_4 and *J*-values are required in order to quantify how the pseudo-first order rate constant for alkyl nitrate loss ($k_B = k_4[OH] + J_{RONO2}$) changes with altitude.

[45] Because the rate constants k_1 and k_4 are known for surface temperatures, photochemical ages can be considered for air masses sampled near the Earth's surface in which the initial alkyl nitrate concentration is known to be zero. Although the Shanghai and Seoul plumes were sampled at low altitude, the initial alkyl nitrate concentration within Shanghai and Seoul was likely not zero (section 4.5.2). As a result, the age of these plumes cannot be accurately quantified based on $RONO_2$/RH ratios. Further, in air samples collected over the western Pacific during the Pacific Exploratory Mission (PEM) West A, *McKeen et al.* [1996] found that dilution was so effective that hydrocarbon ratios should be used as photochemical markers only for hydrocarbons more reactive than *n*-butane (OH lifetime ~ 3 days under PEM-West A conditions). Under TRACE-P conditions the lifetimes of 2-$PeONO_2$ and 3-$PeONO_2$ are 6 and 8 days, respectively, and the lifetime of their parent *n*-pentane is 3–4 days. Therefore for TRACE-P, 2-$PeONO_2$/*n*-pentane and 3-$PeONO_2$/*n*-pentane are not good candidates for use as photochemical markers. Instead, the measured ratios of 2-$PeONO_2$/*n*-pentane vs. 2-$BuONO_2$/*n*-butane for the Shanghai and Seoul plumes have been superimposed on evolution curves that were generated under surface-level conditions only to illustrate the sensitivity of estimated photochemical ages to the amount of OH used in the model (Figures 5a–5b). Under an applied diurnally averaged [OH] of 8.8×10^5 molec cm^3, the predicted photochemical ages of the Shanghai and Seoul plumes are roughly 2–3 days and 4–5 days, respectively (Figure 5a). When the applied [OH] is doubled to 1.76×10^6 molec cm^3, the estimated ages of the Shanghai and Seoul plumes are roughly 1–2 and 2–3 days, respectively (Figure 5b).

[46] Overall, the amount of photochemical processing within an air mass can be quantified using equation (9) but only under strict conditions. The modeled ages are highly sensitive to the amount of OH that is applied, and the model is limited to surface-level conditions. Although knowing the ventilation time of a city may allow the elapsed time (since the parent hydrocarbon was emitted from a polluting source) to be quantified, equation (9) only applies if the alkyl nitrate concentration prior to $t = 0$ was zero. In addition, the influence of dilution must be considered. Whereas sensitivity to initial conditions may not allow equation (9) to be applied quantitatively, it can be used qualitatively to study the relative extent of photochemical processing among different air masses, as discussed below.

4.6.2. Literature Comparison

[47] Alkyl nitrate evolution was modeled using equation (9) and the results were compared with observations from all TRACE-P flights. The newer branching ratios from the literature were used in this analysis. To satisfy the condition of zero initial alkyl nitrate concentrations, air samples displaying large oceanic sources of alkyl nitrates were not used. Because oceans are a major source of $MeONO_2$, ratios of $MeONO_2/RONO_2$ can be much higher in air masses that have recently been at low altitude over the Pacific Ocean compared to those that have been influenced by urban/industrial emissions [*Blake et al.*, 2003]. Blake et al. used ratios of $MeONO_2/EtONO_2$, $MeONO_2$/2-$PrONO_2$, and $MeONO_2$/2-$BuONO_2$ to distinguish between air masses influenced by equatorial oceanic sources and those influenced by northern hemispheric urban/industrial sources. In this study, as in the study by Blake et al., plots of $MeONO_2/EtONO_2$, $MeONO_2$/2-$PrONO_2$, and $MeONO_2$/2-$BuONO_2$ showed clear marine and nonmarine "wings" (data not shown), and the marine wings were removed from the data set. As noted in section 4.1, the influence of the marine source on the TRACE-P alkyl nitrates was less prominent compared with their photochemical source.

[48] The ratio of each daughter alkyl nitrate to its parent hydrocarbon was plotted against 2-$BuONO_2$/*n*-butane using the edited data (Figures 6a–6e). The ratio of 2-$BuONO_2$/*n*-butane is chosen for the abscissa because *n*-butane is one of the most abundant hydrocarbons emitted and because 2-$BuONO_2$ is among the most abundant alkyl nitrates formed [*Roberts et al.*, 1998]. In addition, 2-$BuONO_2$ is not formed in significant quantities from other decomposition pathways [*Roberts et al.*, 1998]. The dark grey triangles in Figure 6 represent TRACE-P field data collected near the surface (0–1 km), and the light grey squares show the remaining data collected between 1 and 12 km. Lower ratios (in the bottom left of each panel) represent fresh emissions, and higher ratios (in the top right of each graph) indicate photochemically processed air. For the surface data, individual points were grouped into bins each containing 10% of the edited data by sorting the data based on 2-$BuONO_2$/*n*-butane ratios. An average ratio is plotted for each bin together with error bars that represent ±1σ. The solid line in each panel is the modeled curve based on equation (9). As discussed in section 4.6.1, equation (9) can only be solved

for surface-level conditions, and the modeled curves shown in Figure 6 represent surface conditions.

[49] The measured $RONO_2$/RH ratios generally lie above the modeled line for C_2-C_3 alkyl nitrates (Figures 6a–6c) and below the modeled line for C_5 alkyl nitrates (Figures 6d–6e). *Bertman et al.* [1995], *Roberts et al.* [1998], and *Stroud et al.* [2001] observed similar results during field studies in Pennsylvania and Alabama, in Nova Scotia, and over

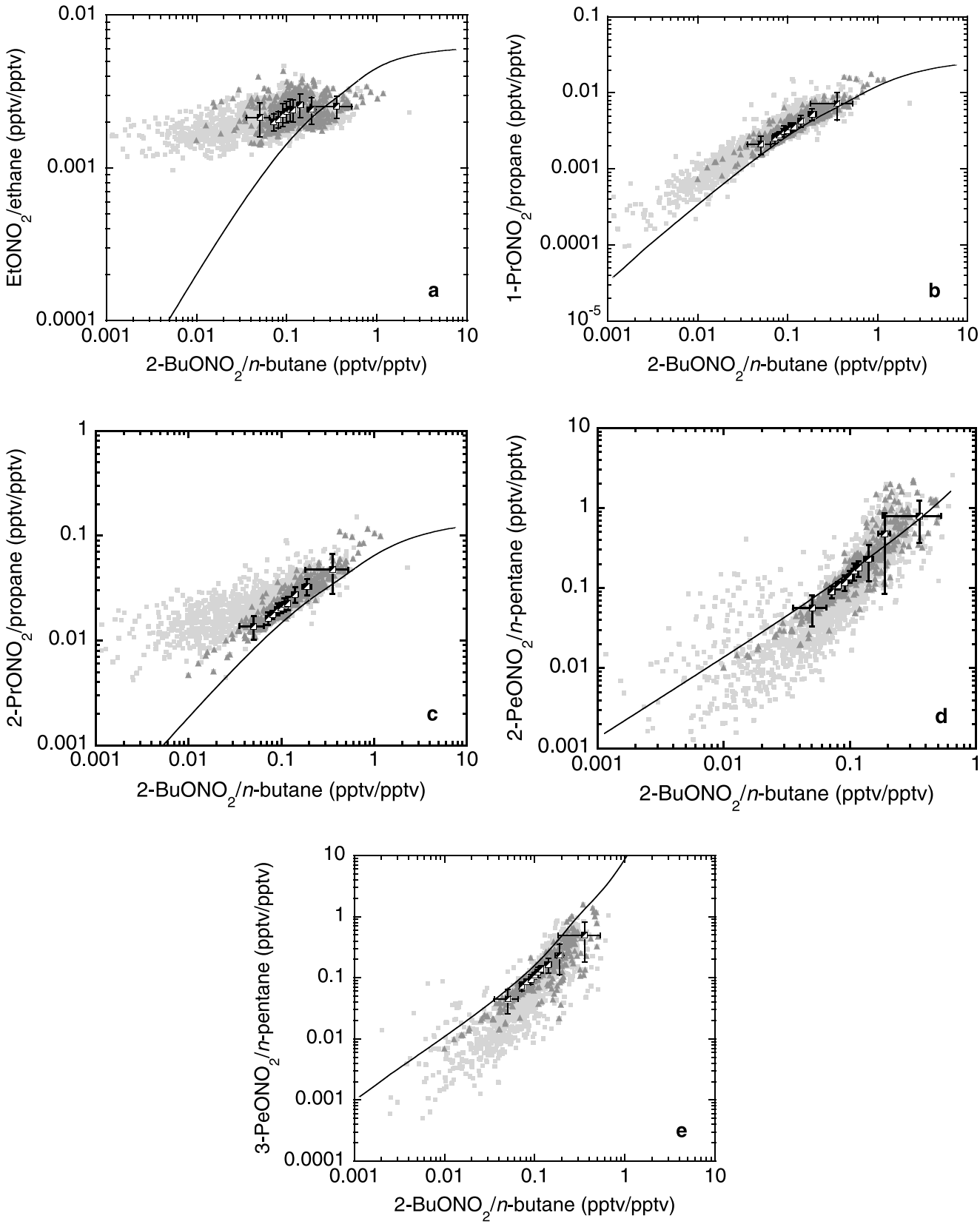

Colorado, respectively, with the exception of pentyl nitrate results from Pennsylvania which lied above the modeled curve, possibly as a result of chromatographic coelution problems. Whereas the C_2-C_3 alkyl nitrates have shorter lifetimes than their parent hydrocarbons, the C_4-C_5 alkyl nitrates have longer lifetimes than their parents [*Roberts et al.*, 1998]. As a result, mixing with older air masses lowers the $RONO_2$/RH ratio for C_2-C_3 alkyl nitrates, and raises the ratio for C_4-C_5 alkyl nitrates. However, similar to findings by *Roberts et al.* [1998], this is opposite to the overall effects that are observed in Figures 6a–6e, in which C_2-C_3 results are larger than predicted whereas C_5 results are smaller than predicted.

[50] The average $EtONO_2$/ethane vs. 2-$BuONO_2$/*n*-butane ratios measured during TRACE-P differ from the modeled curve at short photochemical processing times and show some indication of leveling off at longer residence times, although the scatter in the data are too large to clearly show the approach to a steady state (Figure 6a). By comparison, the $EtONO_2$/ethane vs. 2-$BuONO_2$/*n*-butane ratios from Alabama were about a factor of 10 above the predicted line and were used as a strong indication of additional sources of $EtONO_2$, such as the decomposition of larger alkoxy radicals to form ethyl radicals [*Bertman et al.*, 1995]. Measured ratios from the Nova Scotia field study lied closer to the predicted line and tended towards it at longer photochemical processing times (higher ratios) [*Roberts et al.*, 1998]. Roberts et al. suggested that the difference between the Alabama and Nova Scotia data sets likely arose because the Nova Scotia site (on the eastern edge of the continent) was more often influenced by aged air than the Alabama site. Older air could contain NO_x levels that are below the threshold for $RONO_2$ production, and could mix in air masses with lower $EtONO_2$/ethane ratios. The strong tendency of the TRACE-P data towards the predicted line at longer residence times suggests that these air masses were influenced by mixing with older air masses. The deviation from the line at lower ratios is consistent with an additional source of ethyl radicals, similar to the findings by *Bertman et al.* [1995] and *Roberts et al.* [1998]. The presence of additional $EtONO_2$ precursors is consistent with the unexpectedly high levels of acetaldehyde that were observed during TRACE-P (D. Jacob, Harvard University, personal communication, 2002).

[51] For the surface-level data the slope of 1-$PrONO_2$/propane versus 2-$BuONO_2$/*n*-butane agrees very well with predicted values, with a small (20–30%) offset above the predicted curve (Figure 6b). The largest ratios (oldest air masses) lie closer to the predicted line than smaller ratios, again consistent with mixing with older air masses at longer residence times. However, as with $EtONO_2$/ethane, the scatter of the data is too large to discern a statistically significant trend. By contrast to the TRACE-P results, *Roberts et al.* [1998] observed a factor of 8–10 offset for 1-$PrONO_2$/propane vs. 2-$BuONO_2$/*n*-butane, which they attributed to a possible local source of 1-$PrONO_2$ precursors such as 2-methyl pentane. Similarly, *Stroud et al.* [2001] observed a factor of 2–10 offset above the predicted line. The TRACE-P field measurements do not show a similarly large offset from the predicted line, indicating that impact from additional 1-$PrONO_2$ precursors was not a large factor in air sampled downwind of Asia.

[52] The 2-$PrONO_2$/propane vs. 2-$BuONO_2$/*n*-butane surface-level data points show a small (25–45%) offset above the modeled curve, whereas data collected between 1 and 12 km lie further above the modeled curve for younger air masses and closer to the line for older air masses (Figure 6c). This suggests that the air masses sampled between 1 and 12 km were influenced by additional sources of 2-$PrONO_2$ precursors, which could also help explain the high acetone levels that were observed during TRACE-P (D. Jacob, Harvard University, personal communication, 2002). We note that although the modeled curve was generated for surface conditions, it can be qualitatively compared to measured ratios at higher altitudes. For example, halving k_A and doubling k_B causes the modeled $RONO_2$/RH ratios to shift to lower values but still along the same curve. *Bertman et al.* [1995], *Roberts et al.* [1998], and *Stroud et al.* [2001] found that their field data lied above the predicted line by factors of 2–5, 2–3, and 2–4, respectively.

[53] In contrast to the C_2-C_3 alkyl nitrates, the C_5 alkyl nitrate results generally lie below the predicted line, although the offset is small (5–35%; Figures 6d–6e). *Roberts et al.* [1998] and *Stroud et al.* [2001] also found good agreement between measured and modeled results, with measurements ~50% lower than the predicted curve. Based on similar findings from measurements in Alabama, *Bertman et al.* [1995] suggested that the chemistry of C_4 and C_5 alkyl nitrates is reasonably well understood. Here, the similar results obtained from independent groups sampling over different global source regions suggest that the photochemical sources of 2-butyl-, 2-pentyl-, and 3-pentyl alkyl nitrates are well represented in alkyl nitrate evolution models such as equation (9).

5. Conclusions

[54] The photochemical production and evolution of six C_2-C_5 alkyl nitrates was investigated using selected data from 5500 whole air samples collected downwind of Asia. The airborne samples covered an altitudinal range of 150 m to 12 km and were collected during the NASA TRACE-P experiment (February–April 2001). 2-Propyl nitrate and 2-$BuONO_2$ were the most abundant C_2-C_5 alkyl nitrates, indicating the importance of photochemical (rather than marine) alkyl nitrate production during TRACE-P. Individ-

Figure 6. (opposite) Measured and modeled time evolution of ratios of daughter alkyl nitrates to their parent hydrocarbons versus 2-$BuONO_2$/*n*-butane, for TRACE-P samples that do not show a marine alkyl nitrate source. (a) $EtONO_2$/ethane; (b) 1-$PrONO_2$/propane; (c) 2-$PrONO_2$/propane; (d) 2-$PeONO_2$/*n*-pentane; (e) 3-$PeONO_2$/*n*-pentane. Dark grey triangles are individual TRACE-P samples collected near the surface (0–1 km); light grey squares show the remaining samples collected between 1 and 12 km; black squares are average ratios each containing 10% of the nonmarine TRACE-P data ($\pm1\sigma$ for 2-$BuONO_2$/*n*-butane in the *x*-direction, and $\pm1\sigma$ for the plotted $RONO_2$/RH in the *y*-direction). The solid lines show modeled evolution curves using kinetic data from the literature.

ual alkyl nitrate mixing ratios ranged from clean marine to polluted continental, and mean alkyl nitrate mixing ratios were similar to those measured in and over rural areas of the United States.

[55] The TRACE-P field measurements were compared with model predictions of alkyl nitrate production and evolution. The photochemical production and destruction of 2-$PeONO_2$ and 3-$PeONO_2$ combine in such a way that the ratio of 3-$PeONO_2$/2-$PeONO_2$ is predicted to increase exponentially with time. As a result, young unprocessed air masses were found to be the best candidates for comparing photochemical production rates of C_5 alkyl nitrates with laboratory predictions. In young, highly polluted air masses such as the Shanghai and Seoul plumes, the ratio of 3-$PeONO_2$/2-$PeONO_2$ was 0.60–0.65. These results agree with predicted ratios from older laboratory kinetic studies (0.63–0.66), and they lie in the lower end of the uncertainty range from the most recent laboratory kinetic studies (0.73 ± 0.08).

[56] Modeled photochemical ages based on $RONO_2$/RH ratios are highly sensitive to OH concentration and are expected to be sensitive to altitude, although the dependence on altitude could not be quantified. During TRACE-P, the influence of dilution and non-zero initial alkyl nitrate concentrations precluded the use of $RONO_2$/RH ratios as quantitative photochemical markers.

[57] The photochemical evolution of alkyl nitrates and their parent hydrocarbons was investigated using TRACE-P data that did not show influence from marine alkyl nitrate sources. Marine influence was determined using the ratios of $MeONO_2$/$RONO_2$, which can be much higher in air masses that have recently been at low altitude over the Pacific as compared to air masses influenced by urban/industrial emissions. Evidence for additional Asian sources of $EtONO_2$ and 2-$PrONO_2$ precursors, beyond what is expected from ethane and propane chemistry, was found based on deviations of measured $RONO_2$/RH ratios from modeled evolution curves. The additional $EtONO_2$ and 2-$PrONO_2$ precursors could help to explain the high levels of acetaldehyde and acetone that were observed during TRACE-P. The measured ratios of 1-$PrONO_2$, 2-$PeONO_2$, and 3-$PeONO_2$ to their respective parent hydrocarbons agreed fairly well with model predictions, suggesting little impact by additional precursors from Asian sources.

[58] **Acknowledgments.** We gratefully acknowledge excellent work by the UCI team during the TRACE-P mission (Murray McEachern, Barbara Barletta, John Bilicska, Yunsoo Choi, Lambert Doezema, Kevin Gervais, Lissa Giroux, Max Hoshino, Aaron Katzenstein, Aisha Kennedy, Jimena Lopez, Brent Love, Simone Meinardi, Jason Paisley, Aaron Swanson, Clarissa Whitelaw, and Barbara Yu). We wish to thank Hartwig Harder (Pennsylvania State University), Jung-Hun Woo (University of Iowa), David Streets (Argonne National Laboratory), Alan Fried (NCAR), Ivar Isaksen (University of Oslo), and Ed Browell (NASA-Langley) for helpful discussions and information. We also thank Daniel Jacob (Harvard University) for pointing out the possible implications of the missing $EtONO_2$ and 2-$PrONO_2$ sources on the high levels of acetaldehyde and acetone observed during TRACE-P. The carbon monoxide data are courtesy of Glen Sachse (NASA-Langley), and the hydroxyl data are courtesy of William Brune (Pennsylvania State University). Acetone and acetaldehyde were measured by Hanwant Singh (NASA-Ames) and by Eric Apel (NCAR) and Daniel Riemer (University of Miami).

References

Arey, J., S. M. Aschmann, E. S. C. Kwok, and R. Atkinson, Alkyl nitrate, hydroxyalkyl nitrate, and hydroxycarbonyl formation from the NO_x-Air photooxidations of C_5–C_8 *n*-alkanes, *J. Phys. Chem.*, *105*, 1020–1027, 2001.

Atkinson, R., A structure-activity relationship for the estimation of rate constants for the gas-phase reactions of OH radicals with organic compounds, *Int. J. Chem. Kinet.*, *19*, 799–828, 1987.

Atkinson, R., Gas-phase tropospheric chemistry of organic compounds: A review, *Atmos. Environ.*, *24*, 1–41, 1990.

Atkinson, R., Gas-phase tropospheric chemistry of volatile organic compounds: 1. Alkanes and alkenes, *J. Phys. Chem. Ref. Data*, *26*, 215–290, 1997.

Atkinson, R., S. M. Aschmann, W. P. L. Carter, A. M. Winer, and J. N. Pitts Jr., Alkyl nitrate formation from the NO_x-air photooxidations of C_2–C_8 *n*-alkanes, *J. Phys. Chem.*, *86*, 4563–4569, 1982.

Atkinson, R., S. M. Aschmann, and A. M. Winer, Alkyl nitrate formation from the reaction of a series of branched RO_2 radicals with NO as a function of temperature and pressure, *J. Atmos. Chem.*, *5*, 91–102, 1987.

Atkinson, R., E. S. C. Kwok, J. Arey, and S. M. Aschmann, Reactions of alkoxyl radicals in the atmosphere, *Faraday Discuss.*, *100*, 23–27, 1995.

Atkinson, R., D. L. Baulch, R. A. Cox, R. F. Hampson Jr., J. A. Kerr, M. J. Rossi, and J. Troe, Evaluated kinetic, photochemical and heterogeneous data for atmospheric chemistry: Supplement V. IUPAC subcommittee on gas kinetic data evaluation for atmospheric chemistry, *J. Phys. Chem. Ref. Data*, *26*, 521–1011, 1997.

Atlas, E., and B. A. Ridley, The Mauna Loa Observatory Photochemistry Experiment: Introduction, *J. Geophys. Res.*, *101*, 14,531–14,542, 1996.

Atlas, E., W. Pollock, J. Greenberg, L. Heidt, and A. M. Thompson, Alkyl nitrates, nonmethane hydrocarbons, and halocarbon gases over the equatorial Pacific Ocean during SAGA 3, *J. Geophys. Res.*, *98*, 16,933–16,949, 1993.

Bertman, S. B., J. M. Roberts, D. D. Parish, M. P. Buhr, P. D. Goldan, W. C. Kuster, F. C. Fehsenfeld, S. A. Montzka, and H. Westberg, Evolution of alkyl nitrates with air mass age, *J. Geophys. Res.*, *100*, 22,805–22,813, 1995.

Blake, N. J., D. R. Blake, O. W. Wingenter, B. C. Sive, C. H. Kang, D. C. Thornton, A. R. Bandy, E. Atlas, F. Flocke, and F. S. Rowland, Aircraft measurements of the latitudinal, vertical and seasonal variations of NMHCs, methyl nitrate, and methyl halides during ACE-1, *J. Geophys. Res.*, *104*, 21,803–21,817, 1999.

Blake, N. J., et al., Large-scale latitudinal and vertical distributions of NMHCs and selected halocarbons in the troposphere over the Pacific Ocean during the March-April 1999 Pacific Exploratory Mission (PEM-Tropics B), *J. Geophys. Res.*, *106*, 32,627–32,644, 2001.

Blake, N. J., D. R. Blake, A. L. Swanson, E. Atlas, F. Flocke, and F. S. Rowland, Latitudinal, vertical, and seasonal variations of C_1–C_4 alkyl nitrates in the troposphere over the Pacific Ocean during PEM-Tropics A and B: Oceanic and continental sources, *J. Geophys. Res.*, *108*(D2), 8242, doi:10.1029/2001JD001444, 2003.

Buhr, M., F. C. Fehsenfeld, D. D. Parrish, R. E. Sievers, and J. M. Roberts, Contribution of organic nitrates to the total odd-nitrogen budget at a rural, eastern U.S. site, *J. Geophys. Res.*, *95*, 9809–9816, 1990.

Chuck, A. L., S. M. Turner, and P. S. Liss, Direct evidence for a marine source of C_1 and C_2 alkyl nitrates, *Science*, *297*, 1151–1154, 2002.

Clemitshaw, K. C., J. Williams, O. V. Rattigan, D. E. Shallcross, K. S. Law, and R. A. Cox, Gas-phase ultraviolet absorption cross-sections and atmospheric lifetimes of several C_2–C_5 alkyl nitrates, *J. Photochem. Photobiol. A: Chem.*, *102*, 117–126, 1997.

Colman, J. J., A. L. Swanson, S. Meinardi, B. C. Sive, D. R. Blake, and F. S. Rowland, Description of the analysis of a wide range of volatile organic compounds in whole air samples collected during PEM-Tropics A and B, *Anal. Chem.*, *73*, 3723–3731, 2001.

Crawford, J., et al., Assessment of upper tropospheric HO_x sources over the tropical Pacific based on NASA GTE/PEM data: Net effect on HO_x and other photochemical parameters, *J. Geophys. Res.*, *104*, 16,255–16,273, 1999.

Darnall, K. R., W. P. L. Carter, A. M. Winer, A. C. Lloyd, and J. N. Pitts Jr., Importance of RO_2 + NO in alkyl nitrate formation from C_4–C_6 alkane photooxidations under simulated atmospheric conditions, *J. Phys. Chem.*, *80*, 1948–1950, 1976.

Finlayson-Pitts, B. J., and J. N. Pitts, *Chemistry of the Upper and Lower Atmosphere: Theory, Experiments, and Applications*, 969 pp., Academic, San Diego, Calif., 2000.

Flocke, F., A. Volz-Thomas, and D. Kley, Measurements of alkyl nitrates in rural and polluted air masses, *Atmos. Environ.*, *25*(A), 1951–1960, 1991.

Flocke, F., A. Volz-Thomas, H.-J. Buers, W. Pätz, H.-J. Garthe, and D. Kley, Long-term measurements of alkyl nitrates in southern Germany General behavior and seasonal and diurnal variation, *J. Geophys. Res.*, *103*, 5729–5746, 1998.

Hess, P. G., N. Srimani, and S. J. Flocke, Trajectories and related variations in the chemical composition of the air for the Mauna Loa Observatory during 1991 and 1992, *J. Geophys. Res.*, *101*, 14,543–14,568, 1996.

Jacob, D. J., J. H. Crawford, M. M. Kleb, V. E. Connors, R. J. Bendura, and J. L. Raper, The transport and chemical evolution over the Pacific (TRACE-P) mission: Design, execution, and overview of results, *J. Geophys. Res.*, *108*(D20), 8781, doi:10.1029/2002JD003276, in press, 2003.

Kwok, E. S. S., and R. Atkinson, Estimation of hydroxyl radical reaction rate constants for gas-phase organic compounds using a structure-reactivity relationship: An update, *Atmos. Environ.*, *29*, 1685–1695, 1995.

Logan, J. A., Tropospheric ozone: Seasonal behavior, trends, and anthropogenic influence, *J. Geophys. Res.*, *90*, 10,463–10,482, 1985.

McKeen, S. A., and S. C. Liu, Hydrocarbon ratios and photochemical history of air masses, *Geophys. Res. Lett.*, *20*, 2363–2366, 1993.

McKeen, S. A., S. C. Liu, E.-Y. Hsie, X. Lin, J. D. Bradshaw, S. Smyth, G. L. Gregory, and D. R. Blake, Hydrocarbon ratios during PEM-WEST A: A model perspective, *J. Geophys. Res.*, *101*, 2087–2109, 1996.

Ranschaert, D. L., N. J. Schneider, and M. J. Elrod, Kinetics of the $C_2H_5O_2$ + NO_x reactions: Temperature dependence of the overall rate constant and the $C_2H_5ONO_2$ branching channel of $C_2H_5O_2$ + NO, *J. Phys. Chem. A*, *104*, 5758–5765, 2000.

Ridley, B. A., et al., The behavior of some organic nitrates at Boulder and Niwot Ridge, Colorado, *J. Geophys. Res.*, *95*, 13,949–13,961, 1990.

Roberts, J. M., The atmospheric chemistry of organic nitrates, *Atmos. Environ.*, *24A*, 243–287, 1990.

Roberts, J. M., and R. W. Fajer, UV absorption cross sections of organic nitrates of potential atmospheric importance and estimation of atmospheric lifetimes, *Environ. Sci. Technol.*, *23*, 945–951, 1989.

Roberts, J. M., S. B. Bertman, D. D. Parrish, F. C. Fehsenfeld, B. T. Jobson, and H. Niki, Measurement of alkyl nitrates at Chebogue Point, Nova Scotia during the 1993 North Atlantic Regional Experiment (NARE) intensive, *J. Geophys. Res.*, *103*, 13,569–13,580, 1998.

Shepson, P. B., K. G. Anlauf, J. W. Bottenheim, H. A. Wiebe, N. Gao, K. Muthuramu, and G. I. Mackay, Alkyl nitrates and their contribution to reactive odd nitrogen at a rural site in Ontario, *Atmos. Environ.*, *27A*, 749–757, 1993.

Simpson, I. J., S. Meinardi, D. R. Blake, N. J. Blake, F. S. Rowland, E. Atlas, and F. Flocke, A biomass burning source of C_1–C_4 alkyl nitrates, *Geophys. Res. Lett.*, *29*(24), 2168, doi:10.1029/2002GL016290, 2002.

Smyth, S., et al., Comparison of free tropospheric western Pacific air mass classification schemes for the PEM-West A experiment, *J. Geophys. Res.*, *101*, 1743–1762, 1996.

Streets, D. G., L. Hedayat, G. R. Carmichael, R. L. Arndt, and L. D. Carter, Potential for advanced technology to improve air quality and human health in Shanghai, *Environ. Manage.*, *23*, 279–295, 1999.

Stroud, C. A., et al., Alkyl nitrate measurements during STERAO 1996 and NARE 1997: Intercomparison and survey of results, *J. Geophys. Res.*, *106*, 23,043–23,053, 2001.

Talbot, R. W., J. E. Dibb, E. M. Scheuer, J. D. Bradshaw, S. T. Sandholm, H. B. Singh, D. R. Blake, N. J. Blake, E. Atlas, and F. Flocke, Tropospheric reactive odd nitrogen over the South Pacific in austral Springtime, *J. Geophys. Res.*, *105*, 6681–6694, 2000.

Talukdar, R. K., J. B. Burkholder, M. Hunter, M. K. Gilles, J. M. Roberts, and A. R. Ravishankara, Atmospheric fate of several alkyl nitrates Part 2 UV absorption cross-sections and photodissociation quantum yields, *J. Chem. Soc. Faraday Trans.*, *93*, 2797–2805, 1997.

Walega, J. G., B. A. Ridley, S. Madronic, F. E. Grahek, J. D. Shetter, T. D. Sauvain, C. J. Hahn, J. T. Merrill, B. A. Bodhaine, and E. Robinson, Observations of peroxyacetyl nitrate, peroxyproprionyl nitrate, methyl nitrate and ozone during the Mauna Loa Observatory Photochemistry Experiment, *J. Geophys. Res.*, *97*, 10,311–10,330, 1992.

E. Atlas and F. Flocke, Atmospheric Chemistry Division, National Center for Atmospheric Research, P. O. Box 3000, Boulder, CO 80307-3000, USA. (atlas@ucar.edu; ffl@ucar.edu)

D. R. Blake, N. J. Blake, S. Meinardi, F. S. Rowland, and I. J. Simpson, Department of Chemistry, 516 Rowland Hall University of California-Irvine, Irvine, CA 92697-2025, USA. (drblake@uci.edu; nblake@uci.edu; smeinard@uci.edu; rowland@uci.edu; isimpson@uci.edu)

J. H. Crawford, NASA Langley Research Center, Mail Stop 483, Hampton, VA 23681, USA. (j.h.crawford@larc.nasa.gov)

H. E. Fuelberg and C. M. Kiley, Department of Meteorology, Florida State University, 309 Love Building, Tallahassee, FL 32306, USA. (fuelberg@huey.met.fsu.edu; ckiley@huey.met.fsu.edu)